Progress In Electromagnetics Research, PIER 52, 153–171, 2005

ELECTROMAGETIC SCATTERING MODEL FOR RICE CANOPY BASED ON MONTE CARLO SIMULATION

L. Wang † **and J. A. Kong**

Department of Electrical Engineering and Computer Science
Massachusetts Institute of Technology
Cambridge, MA 02139, USA

K. H. Ding

Air Force Research Laboratory
Sensors Directorate, AFRL/SNHE
Hanscom AFB, MA 01731, USA

T. Le Toan

Centre d'Etudes Spatiales de la BIOsphère (CESBIO)
31401 Toulouse Cedex, France

F. Ribbes-Baillarin

Spot Image
31030 Toulouse Cedex 4, France

N. Floury

ESA-ESTEC
TEC-EEP, PO Box 299
2200-AG Noordwijk. The Netherlands

Abstract—A scattering model for rice canopy based on Monte Carlo simulations is applied to interpret RADARSAT data and to predict the temporal response of rice growth. The model takes into account the coherent wave interactions among vegetative elements which usually occur in clusters with closely spaced elements. The model was also used to analyze the structural effect of rice fields on the scattering

† Also with Lawrence Livermore National Laboratory, L-645, Livermore, CA 94550, USA

returns. Simulation results show a significant difference in L-band backscattering returns from rice fields with different structures, and are consistent with empirical observations from JERS-1 Campaign. Taking the ratio of HH over VV can help eliminating ambiguities in this inverse scattering problem.

1. INTRODUCTION

Rice is an essential food source in many regions of the world such as Asia. It forms the basis of the economy in many countries. Therefore, rice monitoring is economically useful in predicting the yield of rice crops. In addition, rice monitoring is important environmentally. The knowledge of rice growing areas can be used to estimate the flux of methane from the irrigated rice fields to the atmosphere [2]. Methane is second in importance only to carbon dioxide as a greenhouse gas. Flooding a rice field cuts off the oxygen supply from the atmosphere to the soil; methane is the major product in the process.

In recent years, satellite remote sensing has played an important role in most crop monitoring programs. Investigations have been carried out using X-band airborne synthetic aperture radar (SAR) [7]. There have also been some pilot studies that use European Satellite ERS-1 Synthetic Aperture Radar (SAR) data to estimate rice crop acreage and growth at several places in the world such as Japan [4, 5], Thailand [1], and Indonesia [8]. Temporal variations of the radar backscattering coefficients observed by ERS-1 at several test-sites were analyzed to derive a general trend for the response of electromagnetic sensors in a whole growth cycle of rice [8]. It shows a large increase of radar backscatter when the rice plants grow from 0 to 100 days. This large increase can be explained by the increase in biomass and the fact that rice fields have flooded ground surfaces during a large portion of the growing period. Therefore, the increase is enhanced by

this highly reflective underlying flooded surface through the volume-surface interaction. Investigations on the use of satellite data for rice monitoring have also been carried out using the Japanese Earth Satellite-1 (JERS-1) data with the operating frequency at L-band. Rosenqvist, *et al.* pointed out that there is a significant difference in the backscattering results from the rice fields in Niigata, Japan, depending on the planting directions of the rice plants [11]. However, this phenomena was not observed in the backscattering returns from the rice fields in Malaysia as the result of different planting practices between the two countries. Therefore, the structure of the rice fields, that is, how rice plants are planted in the field, can have an important effect on the scattering returns. There were also studies that use the multiple temporal RADARSAT images to monitor the rice growth status [12]. From the RADARSAT data, we recently obtained the rice field scattering returns at two looking angles. To interpret those experimental data and experimental observations such as the effects of the structure of rice fields, a theoretical model which takes into account the distinctive structure of rice plants and the coherent wave interactions among plant elements which are in clusters is needed.

In the past, the electromagnetic scattering returns from the vegetation canopy have been calculated using the radiative transfer theory and the analytic wave theory [13]. The radiative transfer theory is based on the energy transport equation and describes the propagation of specific intensity in the medium. The analytic wave theory starts from Maxwell's equations and incorporates the scattering and absorption characteristics of the medium. More recently, the integral equation formulation with the method of moments computational model has been employed to investigate vegetation scattering [15]. Wave scattering from vegetation has been studied extensively using the radiative transfer approach, which assumes that particles scatter independently. In a previous modeling study [7], rice plants were modeled as thin dielectric cylinders over a rough underlying surface and the backscattering coefficients were obtained using the first order solution of the radiative transfer theory. However, it is important to take into account the coherent wave interactions among vegetative elements of the rice canopy which usually occur in clusters and are closely spaced. Yueh, *et al.* developed a branching model with the wave approach [18]. However, the probability density functions and the pair-distribution functions required in their analytic formulation are usually difficult to obtain for natural vegetation.

Therefore, a coherent scattering model with analytic wave theory is developed based on Monte Carlo simulation for the microwave remote sensing of rice canopy. Unlike the branching model [18], this

scattering model does not require the knowledge of the probability density functions and the pair-distribution functions for the vegetation under interest. Monte Carlo simulation in general is computationally intensive. However, with the rapid advances of computer technology, using Monte Carlo simulation to solve Maxwell's equations for different applications becomes more practical. It has been applied to the calculation of the scattering returns from the rough surface [10], and densely packed spheres [19]. With the Monte Carlo simulation approach, the locations and characteristics of particles are supplied by computer experiments according to the ground truth characterizations. These simulated scenarios are then utilized in solving Maxwell's equations. The simulated results from the developed model has been compared with ERS-1 data which has VV polarization [9]. The comparison shows good agreements between the simulation and the experimental results. In this paper, the simulated results from the developed model can be further validated with the new RADARSAT data which has HH polarization. The model will also be applied to analyze the effects of the structure of rice fields on scattering returns.

This paper is divided into three main sections. In Section 2, a theoretical scattering model from rice canopy based on Monte Carlo simulation is described. Simulation results using the developed model are compared with RADARSAT data at 23° and 43° incident angles in Section 3. In Section 4, the model is applied to investigate the effects of the structure of rice fields on scattering returns. Backscattering results are shown for both L- and C-band frequencies. The ratio of HH over VV versus the age of rice canopy for different cases of rice field structures is also given to show the possibility of using HH/VV to eliminate ambiguities for the inversion problem at L-band.

2. ELECTROMAGNETIC SCATTERING FROM THE RICE PLANTS

In the Monte Carlo simulation approach, the first step is to create simulated scenarios for the vegetation canopy of interest. The configurations are created on the basis of the ground truth characterizations such as the fractional volumes, sizes, and shapes of stems and leaves. Therefore, the location, orientation, and distribution of every vegetation component can be obtained from simulations. In the simulation, rice plants are planted with spacing a in the x direction and spacing b in the y direction over a square area A (Figure 1). Small random variations in the spacing between rice plants are also considered. Each rice plant contains a bunch of N_s vertical dielectric cylindrical stems with height H, radius c, and complex dielectric

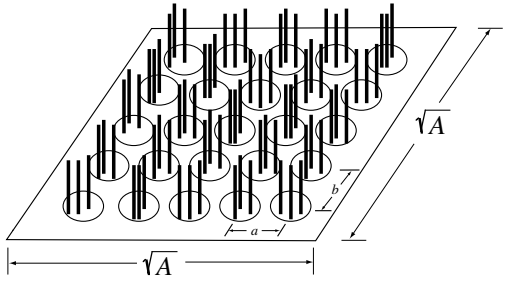

Figure 1. Configuration for the scattering model from a rice field. Rice plants are planted with spacing a in the x direction and spacing b in the y direction over a square area A. Within a rice bunch, the stems are randomly placed inside a circle with uniform distribution.

constant ϵ_s. Each rice stem has N_ℓ leaves of elliptical disc shape with length ℓ, width w, thickness d, and complex dielectric constant ϵ_ℓ. Within a rice bunch, the stems are randomly placed inside a circle of radius c_b with uniform distribution [14]. There are N_c bunches such that the total number of stems in the rice canopy is $N_c \times N_s$ and the total number of leaves is $N_c \times N_s \times N_\ell$. The height of the stems are also generated randomly with Gaussian distribution given the mean and the standard deviation of the height. The lower half space is water, with complex dielectric constant ϵ_1.

Consider a configuration of a rice field where the top of the rice canopy is indicated by $z = 0$ and the boundary between the rice canopy and the ground (water in our case) is $z = -h$. Given the configuration of the rice field and an incident wave $\bar{E}^i$ in the direction (θ_i, ϕ_i), the first-order solution of the backscattered electric field can be expressed as the sum of four terms which describes the four major scattering mechanisms in a rice canopy (Figure 2).

$$E_q^s(\bar{r}) = \frac{e^{ikr}}{r}\left(S_1 + S_2 + S_3 + S_4\right) E_p^i \tag{1}$$

where q and p are the polarization components (q, p = h or v) of the scattered and incident waves, respectively.

S_1 describes the the direct scattering from a particle (Figure 2a) and can be expressed as

$$S_1 = \sum_{\substack{t=\text{stem} \\ \text{or leaf}}} \sum_{j=1}^{N_t} f_{qp}^t(\pi - \theta_i, \pi + \phi_i; \theta_i, \phi_i) e^{i[\bar{k}_p^i(\theta_i,\phi_i) - \bar{k}_q^s(\pi-\theta_i,\pi+\phi_i)]\cdot\bar{r}_j^t} \tag{2}$$

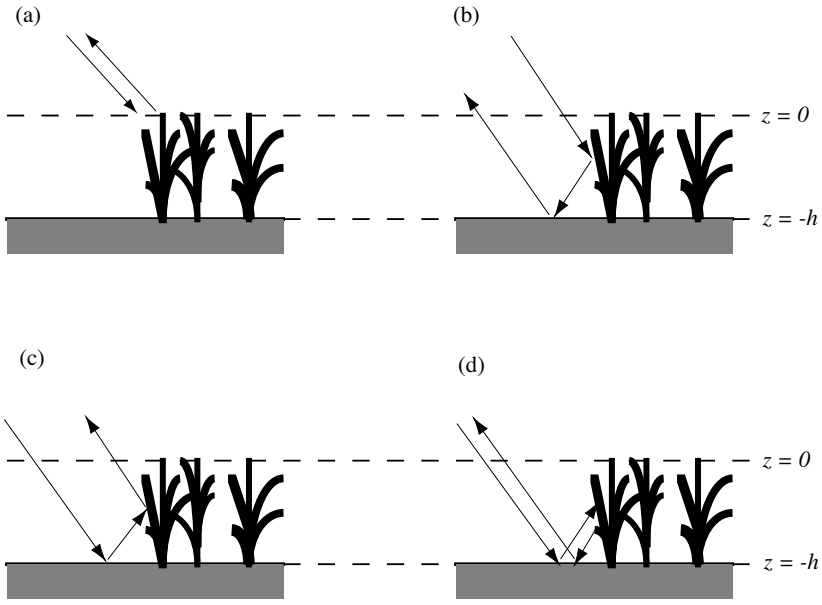

Figure 2. Four major scattering mechanisms in the rice canopy: (a) direct scattering from scatterers, (b) single scattering from the scatterer followed by reflection off the boundary, (c) surface scattering followed by single scattering, (d) reflection by the boundary followed by single scattering from the scatterer and further followed by reflection off the boundary.

where t is the index for the scatterer type—stem or leaf, $N_t = N_c \times N_s$ for stems, and $N_c \times N_s \times N_\ell$ for leaves. f_{qp}^t is the scattering matrix element. $\bar{k}_p^i$ is the propagation vector of the incident wave, $\bar{k}_q^s$ is the propagation vector of the backscattered field. $\bar{r}_j^t = \hat{x}x_j^t + \hat{y}y_j^t - \hat{z}z_j^t$ is the location of the element j of type t.

The second term S_2 is a single scattering from the scatterer followed by a reflection off the boundary (Figure 2b).

$$S_2 = \sum_{\substack{t=\text{stem} \\ \text{or leaf}}} \sum_{j=1}^{N_t} R_q(\theta_i) f_{qp}^t(\theta_i, \pi + \phi_i; \theta_i, \phi_i) e^{i[\bar{k}_p^i(\theta_i,\phi_i) - \bar{k}_q^s(\theta_i,\pi+\phi_i)]\cdot\bar{r}_j^t} \quad (3)$$

The third term is the reverse of the second term; *i.e.,* it represents

surface scattering followed by single scattering (Figure 2c).

$$S_3 = \sum_{\substack{t=\text{stem} \\ \text{or leaf}}} \sum_{j=1}^{N_t} f_{qp}^t(\pi-\theta_i, \pi+\phi_i; \pi-\theta_i, \phi_i) R_p(\theta_i) e^{i[\bar{k}_p^i(\pi-\theta_i,\phi_i) - \bar{k}_q^s(\pi-\theta_i,\pi+\phi_i)]\cdot\bar{r}_j^t} \tag{4}$$

$R_p(\theta_i)$ and $R_q(\theta_i)$ are the Fresnel reflection coefficients.

The fourth term S_4 describes a reflection by the boundary followed by a single scattering from the particle and further followed by a reflection off the boundary (Figure 2d).

$$S_4 = \sum_{\substack{t=\text{stem} \\ \text{or leaf}}} \sum_{j=1}^{N_t} R_q(\theta_i) f_{qp}^t(\theta_i, \pi+\phi_i; \pi-\theta_i, \phi_i) R_p(\theta_i) e^{i[\bar{k}_p^i(\pi-\theta_i,\phi_i) - \bar{k}_q^s(\theta_i,\pi+\phi_i)]\cdot\bar{r}_j^t} \tag{5}$$

For stems, the scattering is calculated using the finite cylinder approximation [3] in which the induced current in the dielectric cylinder is assumed to be the same as that of the infinitely long cylinder of the same radius. For leaves, the returns are calculated using the physical optics approximation for elliptic discs [6], which assumes the internal field inside the disc to be the same as that of the infinitely extended dielectric layer of the same thickness. The effects of attenuation on the coherent wave caused by the inhomogeneities are also taken into account using Foldy's approximation [18]. The attenuation is obtained by averaging the forward scattering returns of each scattering component. The canopy components are assumed to be excited by this coherent wave. The two characteristic waves propagate along the direction (θ, ϕ) inside the rice canopy with the propagation constants

$$k_h = k_0 - iM_{hh} \tag{6}$$

$$k_v = k_0 - iM_{vv} \tag{7}$$

for horizontally and vertically polarized components, respectively. In Equations (6) and (7),

$$M_{qp} = \frac{i2\pi}{k_0} \frac{N_c N_s}{Ah} \left(\left\langle f_{qp}^{\text{stem}}(\theta, \phi; \theta, \phi) \right\rangle + N_\ell \left\langle f_{qp}^{\text{leaf}}(\theta, \phi; \theta, \phi) \right\rangle \right) \tag{8}$$

where the angular brackets denote configurational average, h is the height of the vegetation canopy, and k_0 is the wavenumber of free space. Since the calculated k_h and k_v are quite close to k_0, the effects

of reflection and refraction at the top boundary of the rice canopy layer are neglected here. Based on Equations (6) and (7), Equation (1) can be expressed as

$$\begin{aligned} E_q^s(\bar{r}) &= \frac{e^{ikr}}{r} \sum_{\substack{t=stem \\ or\ leaf}} \sum_{j=1}^{N_t} \Big[f_{qp}^t(\pi-\theta_i, \pi+\phi_i; \theta_i, \phi_i) \\ &\quad \times e^{-M_{qq}\frac{z_j^t}{\cos\theta_i}} e^{-M_{pp}\frac{z_j^t}{\cos\theta_i}} e^{2i(k_x^i x_j^t + k_y^i y_j^t - k_z^i z_j^t)} \\ &+ R_q(\theta_i) f_{qp}^t(\theta_i, \pi+\phi_i; \theta_i, \phi_i) e^{M_{qq}\frac{2h+z_j^t}{\cos\theta_i}} \\ &\quad \times e^{-M_{pp}\frac{z_j^t}{\cos\theta_i}} e^{2i(k_x^i x_j^t + k_y^i y_j^t + k_z^i h)} \\ &+ f_{qp}^t(\pi-\theta_i, \pi+\phi_i; \pi-\theta_i, \phi_i) R_p(\theta_i) \\ &\quad \times e^{-M_{qq}\frac{z_j^t}{\cos\theta_i}} e^{M_{pp}\frac{2h+z_j^t}{\cos\theta_i}} e^{2i(k_x^i x_j^t + k_y^i y_j^t + k_z^i h)} \\ &+ R_q(\theta_i) f_{qp}^t(\theta_i, \pi+\phi_i; \pi-\theta_i, \phi_i) R_p(\theta_i) \\ &\quad e^{M_{qq}\frac{2h+z_j^t}{\cos\theta_i}} e^{M_{pp}\frac{2h+z_j^t}{\cos\theta_i}} e^{2i(k_x^i x_j^t + k_y^i y_j^t + k_z^i (2h+z_j^t))} \Big] E_p^i \end{aligned} \quad (9)$$

where $k_x^i = k_0 \sin\theta_i \cos\phi_i$, $k_y^i = k_0 \sin\theta_i \sin\phi_i$, and $k_z^i = k_0 \cos\theta_i$. The attenuation is from the real part of M_{pp} and M_{qq}. The coherent addition method is adopted in which the total scattered field from the canopy is obtained by adding the scattered field from each component coherently.

The backscatter from the rice canopy is calculated with Monte Carlo simulations. In each realization of the rice field, the center positions of N_c rice clusters are first created and then the positions of the N_s stems within every bunch are generated using a random number generator with a uniform distribution. The positions of rice stems are checked so that there is no overlap between stems. The positions and orientations of the attached leaves on each stem are also generated randomly. The scattered electric field E_s from each realization is calculated according to (5). The backscattering coefficient is then computed from

$$\sigma_{qp} = \frac{4\pi r^2}{A} \frac{< |E_q^s|^2 >}{|E_p^i|^2} \quad (10)$$

where A is the illuminated area. The results are obtained by averaging over an ensemble of realizations. The convergence of the Monte Carlo simulation is demonstrated numerically with respect to the number of scatterers and realizations.

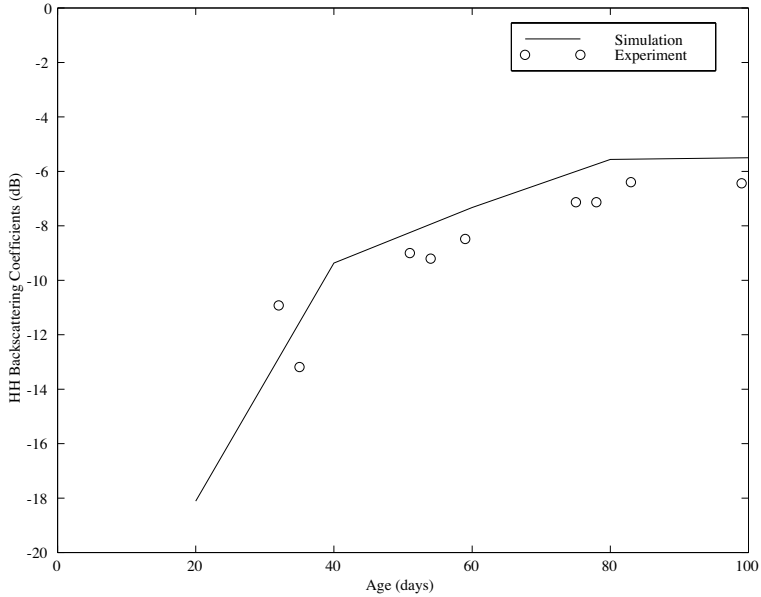

Figure 3. Comparison between the simulated HH backscattering coefficients and RADARSAT data as a function of rice age. The frequency is at C-band and the incident angle is 23°.

Table 1. Input parameters for the simulation of backscattering coefficients of a rice field.

age (days)	20	40	60	80	100
height H (cm)	11.2	26.3	43.6	61.0	76.7
stem radius c (cm)	0.11	0.15	0.18	0.21	0.23
# stems per bunch N_s	3	6	13	20	24
# bunches N_c/A (m^{-2})	9	9	9	9	9
gravimetric water content	0.71	0.77	0.80	0.80	0.75
dielectric constant ϵ_s, ϵ_ℓ	(25.7,8.1)	(29.6,9.2)	(31.7,9.8)	(31.7,9.8)	(28.3,8.8)
leaf width w (cm)	0.43	0.78	1.06	1.3	1.34
leaf length ℓ (cm)	11.75	21.89	30.44	40	40.5
leaf thickness d (cm)	0.02	0.02	0.03	0.03	0.03
# leaves per stem N_ℓ	3	3	4	5	5
stem mean tilt angle θ_{ms} (deg)	0	2	7	11	11
leaf mean tilt angle $\theta_{m\ell}$ (deg)	0	7	14	20	25

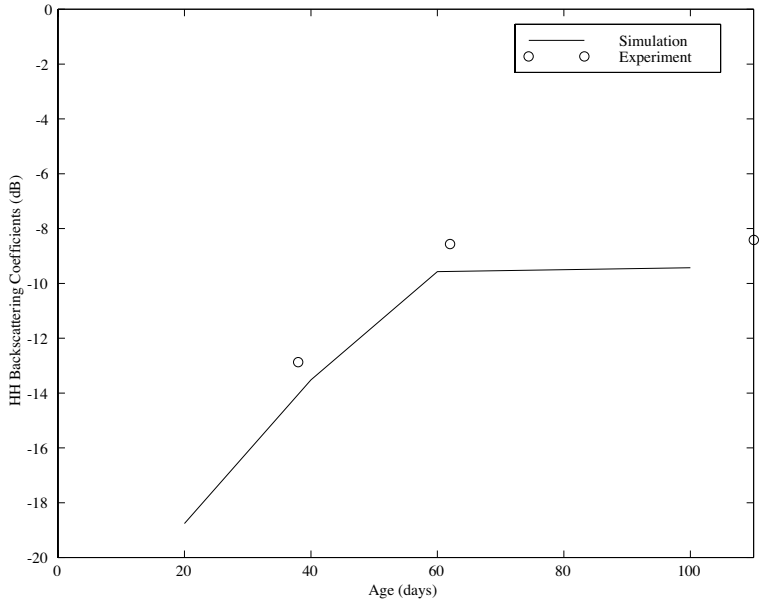

Figure 4. Comparison between the simulated HH backscattering coefficients and RADARSAT data as a function of rice age. The frequency is at C-band and the incident angle is 43°.

3. COMPARISON WITH RADARSAT DATA

The simulated backscattering results at different growth stages are compared with the RADARSAT data. The operating frequency is at C-band (5.3 Ghz), and there is only one polarization, HH. Data were obtained at two incident angles, 23 and 43 degrees. The parameters used in the simulation are determined either directly from the measurements obtained during the experiment or from the existing literature, mainly from IRRI [2]. The parameters used in the simulation of backscattering coefficients of rice fields are summarized in Table 1. The dielectric constants of rice plants at various growth stages are calculated from the gravimetric water content with an empirical formula [17]. Since the bottom part of the rice plants is in the water, the dielectric constant of the surface is that of water at the frequency of 5.3 Ghz at 20°, which is $\epsilon_1 = (74, 21)$ [16]. In the simulation, the average spacing between two rice bunches is about 25 cm. We also assume that the height of stem has a normal distribution with the standard deviation of 1 cm. The backscattering coefficients are obtained by averaging over 50 realizations.

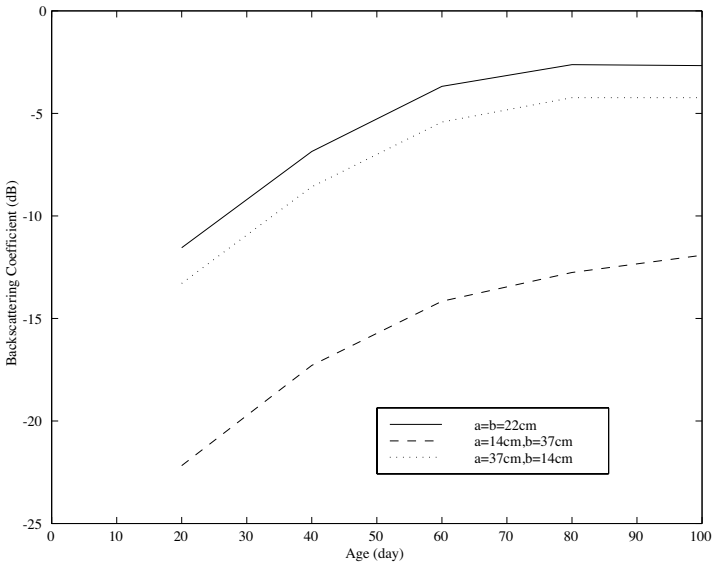

Figure 5. Simulated temporal variation of the L-band backscattering returns assuming the looking direction of the radar to be the x-direction. Simulated cases include fields with equal spacing between rice plants ($a = b = 22\,\text{cm}$), fields with spacings $a = 14\,\text{cm}$ and $b = 37\,\text{cm}$, and fields with spacings $a = 37\,\text{cm}$ and $b = 14\,\text{cm}$.

In Figure 3, the simulated HH backscattering returns at 23° incident angle are compared with the RADARSAT data for different growth stages. The comparison shows good agreements between the simulation results and experimental data. The increasing trend of the temporal radar response is well described by the modeling results. The backscattering returns are mainly from the volume-surface interactions. Since the bottom of rice plants are immersed in water, the contribution of the second, third and fourth scattering mechanisms described in Section 2 to the total scattering from the rice canopy is very large compared to the case of other vegetation fields. Figure 4 shows the temporal response of HH backscattering coefficients when the incident angle is 43 degrees. The result shows a trend similar to the case of 23 degrees except that there is only a very small increase in backscattering coefficients at higher growth stages. This is as expected because the attenuation caused by inhomogeneities in the medium is larger at the 43° incident angle than that at the 23° incident angle. This effect is more dominant at higher growth stages when the stems and leaves become larger.

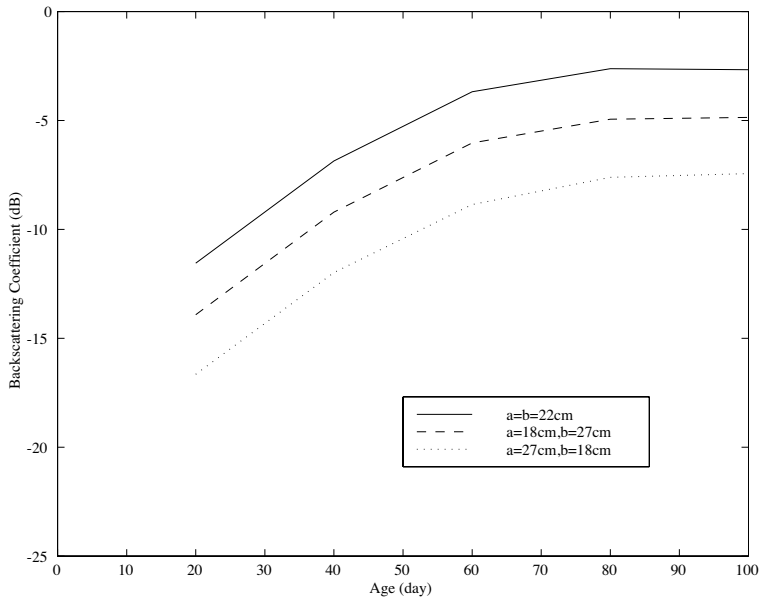

Figure 6. Simulated temporal variation of the L-band backscattering returns assuming the looking direction of the radar to be the x-direction. Simulated cases include fields with equal spacing between rice plants ($a = b = 22\,\text{cm}$), fields with spacings $a = 18\,\text{cm}$ and $b = 27\,\text{cm}$, and fields with spacings $a = 27\,\text{cm}$ and $b = 18\,\text{cm}$.

4. STRUCTURE OF RICE FIELDS

The scattering returns from the rice fields in Niigata, Japan acquired by JERS-1, which operated at L-band (1.25 Ghz) with the incident angle of 35 degrees and one polarization HH, show that the structure of rice fields has a large effect on the returns. Rice cultivation practices in Japan are different from those in Malaysia. Planting is performed by mechanical planting devices mounted on the back of small tractors [11]. The spacing between rice plants in one direction can be very different from the spacing in the other direction. A question was raised in the paper regarding the planting direction which results in a higher scattering return. With the developed model and input parameters [9], the dependence of radar backscattering returns on the geometric properties of the fields is investigated.

Assuming that the looking direction of the radar is in the x-direction and that the area is the same for all fields, the field structures considered include the following cases.

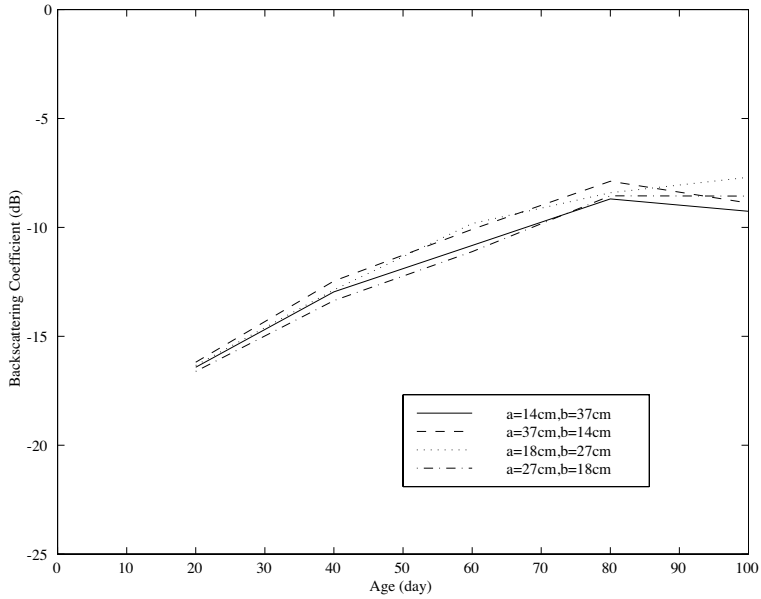

Figure 7. Simulated temporal variation of the C-band backscattering returns assuming the looking direction of the radar to be the x-direction. Simulated cases include fields with spacings $a = 14\,\text{cm}$ and $b = 37\,\text{cm}$, fields with spacings $a = 37\,\text{cm}$ and $b = 14\,\text{cm}$, fields with spacings $a = 18\,\text{cm}$ and $b = 27\,\text{cm}$, and fields with spacings $a = 27\,\text{cm}$ and $b = 18\,\text{cm}$.

1. fields with equal spacing between rice plants ($a = b = 22\,\text{cm}$)
2. fields with spacings $a = 14\,\text{cm}$ and $b = 37\,\text{cm}$
3. fields with spacings $a = 37\,\text{cm}$ and $b = 14\,\text{cm}$
4. fields with spacings $a = 18\,\text{cm}$ and $b = 27\,\text{cm}$
5. fields with spacings $a = 27\,\text{cm}$ and $b = 18\,\text{cm}$

a and b are the spacings in the x and y directions, respectively (Figure 1).

Figure 5 shows the simulated temporal variation of the L-band backscattering returns for cases 1 to 3. The overall shapes of the temporal curves are similar for all three cases. Compared to case 3, the backscattering return is about 8 dB lower for case 2 where a, the spacing in the radar looking direction, is smaller than spacing b in the direction perpendicular to the radar looking direction. The simulated L-band backscattering returns versus rice age for cases 1, 4 and 5 are given in Figure 6. Again, the overall shapes of the temporal

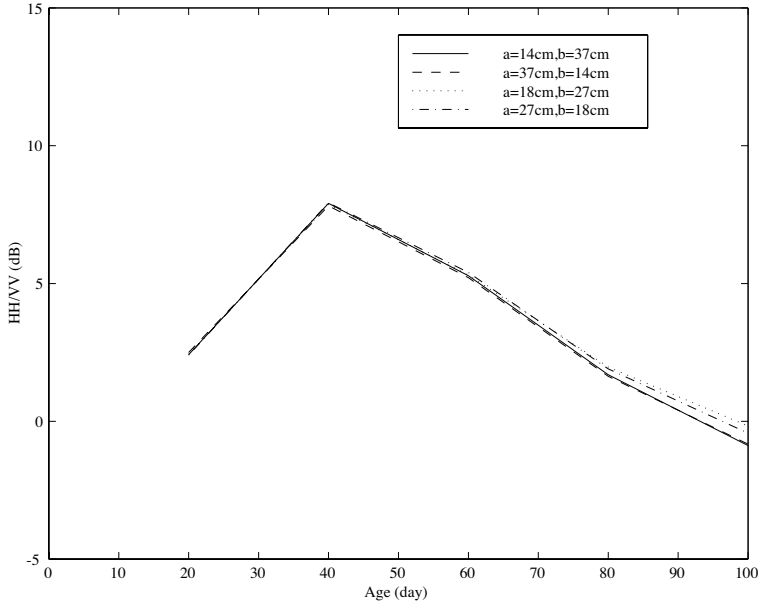

Figure 8. Simulated temporal variation of the ratio of L-band co-pol backscattering coefficients, HH over VV, assuming the looking direction of the radar to be the x-direction. Simulated cases include fields with spacings $a = 14\,\text{cm}$ and $b = 37\,\text{cm}$, fields with spacings $a = 37\,\text{cm}$ and $b = 14\,\text{cm}$, fields with spacings $a = 18\,\text{cm}$ and $b = 27\,\text{cm}$, and fields with spacings $a = 27\,\text{cm}$ and $b = 18\,\text{cm}$.

curves are similar for all three cases. However, compare to case 5, the backscattering return is about 4 dB higher for case 4 where spacing a is smaller than spacing b. Therefore, it is not necessarily true that scattering returns are higher when the spacing in the radar looking direction is smaller than the spacing in the perpendicular direction. The magnitude of scattering returns depends on whether we have a constructive or destructive interference between rice plants, which is related to the spacing between the plants. With a large difference in the backscattering results because of the different structures of the rice fields, inversion will be difficult without the measurements on the plant spacings. However, we can expect less effect of the rice field structure on the returns since the wavelength at C-band is about 6 cm compared to 24 cm at L-band. Figure 7, which shows simulated temporal variations of the C-band backscattering results for cases 2 to 5 described above, confirms this point. The variations in backscattering returns are small for different directions and plant spacings.

If an L-band data set has both HH and VV polarizations, one possible way to perform the inversion without the measurements on the plant spacings is by taking the ratio of HH over VV. The plot of the L-band ratio versus the age of rice canopy for different plant spacings is shown in Figure 8. For the first 95 days, HH backscattering returns are higher than the VV returns since the dominant scattering mechanism is the volume-surface interactions. The reflection coefficient of the horizontal polarization is higher than that of the vertical polarization. The ratios have a decreasing trend after 40 days because the attenuation increases. With water as the underlying surface, the plot for the ratio of HH over VV is different from that of other types of vegetation. The ratio of HH over VV can therefore be utilized for the classification of the rice canopy. The results are very close for different spacing between rice plants. Taking the ratio has the effect of canceling out the phase interactions from the structure of the rice field and provides a useful parameter for the inversion of rice biomass.

5. SUMMARY

A coherent scattering model from rice canopy based on Monte Carlo simulations has been developed, taking into account the structures of rice plants and rice fields and the coherence or phase interference between vegetative elements. It is applied to interpret the RADARSAT data at two incident angles and to analyze the structural effect of rice fields on the scattering returns. The comparison between the simulation results and RADARSAT data shows good agreement for incident angles at 23° and 43°. Because the lower portion of rice plants is immersed in water, the scattering returns are mainly from the volume-surface interactions.

Simulations were also performed using this scattering model to interpret the returns at different growth stages for various structures of rice fields. The result shows that at L-band, the variation in the scattering returns from rice fields with different structures can be large because of constructive and destructive interferences between rice plants as the result of different plant spacings. Without knowing the plant spacing, inversion of rice biomass from the scattering results will be difficult at L-band. For C-band, rice field structure has less effect on the returns because the wavelength at C-band is about 6 cm compared to 24 cm at L-band. However, if the L-band data has both HH and VV polarizations, taking the ratio of HH over VV has the effect of canceling out the phase interactions from the structures of rice fields and is useful for the inversion of biomass.

ACKNOWLEDGMENT

This work was partially supported by NASA contract No. 958461.

REFERENCES

1. Aschbacher, J., A. Pongsrihadulchai, S. Karnchanasutham, C. Rodprom, D. R. Paudyal, and T. Le Toan, "Assessment of ERS-1 data for rice crop mapping and monitoring," *Proceedings of the International Geoscience and Remote Sensing Symposium,* 2183–2185, Florence, Italy, July 1995.
2. IRRI, 1993–1995 IRRI Rice Almanac, International Rice Research Institute, Philippines, 1995.
3. Karam, M. A., A. K. Fung, and Y. M. M. Antar, "Electromagnetic wave scattering from some vegetation samples," *IEEE Transactions on Geoscience and Remote Sensing,* Vol. 26, No. 6, 799–808, 1988.
4. Kurosu, T., T. Suitz, and T. Moriya, "Rice crop monitoring with ERS-1 SAR: a first year result," *Proceedings of the Second ERS-1 Symposium,* Vol. 1, 97–101, Hamburg, Germany, October, 1993.
5. Kurosu, T., M. Fujita, and K. Chiba, "Monitoring of rice crop growth from space using the ERS-1 C-band SAR," *IEEE Transactions on Geoscience and Remote Sensing,* Vol. 33, 1092–1096, 1995.
6. Le Vine, D. M., A. Schneider, R. H. Lang, and H. G. Carter, "Scattering from thin dielectric disks," *IEEE Transactions on Antennas and Propagation,* Vol. 33, No. 12, 1410–1413, 1985.
7. Le Toan, T., H. Laur, E. Mougin, and A. Lopes, "Multitemporal and dual-polarization observations of agricultural vegetation covers by X-band SAR images," *IEEE Transactions on Geoscience and Remote Sensing,* Vol. 27, No. 6, 709–718, 1989.
8. Le Toan, T., F. Ribbes, N. Floury, L. Wang, K. H. Ding, C. C. Hsu, and J. A. Kong, "On the retrieval of rice crop parameters from SAR data," *Proceedings of International Symposium on the Retrieval of Bio- and Geophysical Parameters from SAR Data for Land Applications*, 233–243, Toulouse, France, October 1995.
9. Le Toan, T., F. Ribbes, L. Wang, N. Floury, K. H. Ding, J. A. Kong, N. Fujita, and T. Kurosu, "Rice crop mapping and monitoring using ERS-1 data based on experiment and modeling results," *IEEE Transactions on Geoscience and Remote Sensing,* Vol. 35, No. 1, 41–56, 1997.
10. Pak, K., L. Tsang, C. H. Chan, and J. Johnson, "Backscattering

enhancement of electromagnetic waves from 2-D perfectly conducting random rough surfaces based on Monte Carlo simulations," *Journal of the Optical Society of America A (Optics, Image Science and Vision),* Vol. 12, 2491–2499, 1995.

11. Rosenqvist, Å. and H. Oguma, "Phenological characteristics of cultivated vegetation covers in JERS-1 and ERS-1 synthetic aperture radar data," *Proceedings of International Symposium on Vegetation Monitoring,* 194–198, Japan, August 1995.
12. Shao, Y., C. Wang, X. Fan, and H. Liu, "Estimation of rice growth status using RADARSAT data," *Proceedings of the International Geoscience and Remote Sensing Symposium,* 1430–1432, Singapore, August 1997.
13. Tsang, L., J. A. Kong, and R. T. Shin, *Theory of Microwave Remote Sensing,* Wiley-Interscience, New York, 1985.
14. Tsang L., K.-H. Ding, G. Zhang, C. C. Hsu, and J. A. Kong, "Backscattering enhancement and clustering effects of randomly distributed dielectric cylinders overlying a dielectric half space based on Monte-Carlo simulations," *IEEE Transactions on Antennas and Propagation,* Vol. 43, No. 5, 488–499, 1995.
15. Tsang, L., J. A. Kong, K. H. Ding, and C. O. Ao, *Scattering of Electromagnetic Waves: Numerical Simulations,* Wiley-Interscience, New York, 2001.
16. Ulaby, F. T., R. K. Moore, and A. K. Fung, *Microwave Remote Sensing, Active and Passive,* Vol. III, Artech House, 1986.
17. Ulaby, F. T. and M. A. El-Rays, "Microwave dielectric spectrum of vegetation—part II: dual-dispersion model," *IEEE Transactions on Geoscience and Remote Sensing,* Vol. 25, No. 5, 550–557, 1987.
18. Yueh, S. H., J. A. Kong, J. K. Jao, R. T. Shin, and T. Le Toan, "Branching model for vegetation," *IEEE Transactions on Geoscience and Remote Sensing,* Vol. 30, No. 2, 390–402, 1992.
19. Zurk, L. M., L. Tsang, K. H. Ding, and D. P. Winebrenner, "Monte Carlo simulations of the extinction rate of densely packed spheres with clustered and non-clustered geometries," *Journal of the Optical Society of America A (Optics, Image Science and Vision),* Vol. 12, 1772–1781, 1995.

Li-Fang Wang received the B.S. and M.S. degrees in electrical engineering from Massachusetts Institute of Technology, Cambridge, in 1990 and 1992. She is currently a Ph.D. candidate in electrical engineering at the same university. Since 1997, she has been an

engineer at the Electronics Engineering Directorate of Lawrence Livermore National Laboratory in Livermore, CA. Her research interests include remote sensing , wave scattering from random media, computational electromagnetics, and linear accelerator technology.

Jin Au Kong is a Professor of electrical engineering at Massachusetts Institute of Technology, and President of The Electromagnetics Academy. He has published over 30 books, including Electromagnetic Wave Theory by Wiley Interscience and later EMW Publishing Company, over 600 papers and book chapters. He is the Editor-in-Chief of the Journal of electromagnetic Waves and Applications, Chief Editor of the book series Progress in Electromagnetic Research, and Editor of the Wiley series in remote sensing. His research interests include electromagnetic wave theory and applications.

Kung-Hau Ding is currently a research engineer at the Sensors Directorate of Air Force Research Laboratory in Hanscom Air Force Base, MA, USA. He earned the B.S. degree in Physics from National Tsing-Hua University, Hsinchu, Taiwan, and the MS degrees in Physics and Electrical Engineering, and the Ph.D. degree in Electrical Engineering from University of Washington, Seattle, WA, USA. Upon completion of the PhD in 1989, he worked as a physical scientist, from 1989 to 1993, with the Physical Science Laboratory, New Mexico State University, Las Cruces, NM, USA, and as a research scientist, from 1993 to 1998, with the Research Laboratory of Electronics, Massachusetts Institute of Technology, Cambridge, MA, USA. His research interests include wave propagation and scattering in random media, microwave remote sensing, and radar clutter and target characterizations. He is a member of the Electromagnetics Academy, and IEEE.

Thuy Le Toan received the Engineer degree and the Ph.D. degree in Nuclear Physics from the Paul Sabatier University, Toulouse, France. Since 1973, her research activity has been in the area of microwave remote sensing applied to natural surfaces. Her research interests include experimentation and modeling of microwave interaction with agricultural and forested media, and analysis of SAR images. Since January 1995, she joins the CESBIO where she is presently one of the three group leaders. She has been a Project Coordinator and Principal Investigator of several European SAR projects. She has also been involved in numerous studies for the E.U., ESA, NASA, JAXA and national organizations on the modeling of SAR data and the use of SAR in applications.

Florence Ribbes-Baillarin graduated from Ecole Spérieure d'Agriculture de Purpan in Toulouse, France, with a specialization in Remote Sensing and Biosphere Observation (MScs degree) from Paul Sabatier University. She received the Ph.D. degree on radar remote sensing of vegetation at the Centre dEtudes Spatiales de la Biospheère (CESBIO) in 1998. Since May 2000, she has been working at the Direction of Applications and Development at Spot Image, as an expert in Application Development and Radar satellite data. She has now a 10-year experience in the remote sensing field, especially in radar sensors and operational applications using satellite data such as agriculture, forestry and natural hazards.

Nicolas Floury received the engineering degree in telecommunications from the Ecole Nationale Supérieure des Télécommunications, Paris, in 1993 and the Ph.D. degree in physics applied to remote sensing from Université Paris 7 in 1999. Between 1994 and 1999 he was with CESBIO, Toulouse, France. Since 1999, he has been with the "Wave Propagation and Interaction" group, European Space Research and Technology Center (ESA-ESTEC). His main interests are in electromagnetic modeling and signal processing applied to the study of the interaction between microwaves and natural surfaces.